THE UNIVERSITY OF
WARWICK

Methylthiolate-induced reconstruction of Ag(111): a medium energy ion scattering study

G. S. Parkinson, A. Hentz[+], P. D. Quinn, A. J. Window, D. P. Woodruff[*]

Physics Department, University of Warwick, Coventry CV4 7AL, UK

P. Bailey, T. C. Q. Noakes

CLRC Daresbury Laboratory, Daresbury, Warrington WA4 4AD, UK

Abstract

Medium energy ion scattering (MEIS), using 100 keV H^+ incident ions, has been used to investigate the structure of the $Ag(111)(\sqrt{7}x\sqrt{7})R19°$-$CH_3S$ surface phase. The results provide the first *direct* evidence that this structure does involve substantial reconstruction of the Ag surface layer. The measured absolute scattered ion yields and blocking curves are in generally good agreement with a specific structural model of the surface based on a reconstructed layer containing 3/7 ML Ag atoms, previously suggested on the basis of scanning tunnelling microscopy (STM) and normal incidence X-ray standing wave (NIXSW) studies. However, the MEIS data indicate that any rumpling of the thiolate layer, is small, and probably ≤ 0.2 Å. This value is smaller than the amplitude suggested in the STM and NIXSW studies, but could be entirely consistent with the earlier experimental data.

[+] permanent address Universidade Federal do Rio Grande do Sul, Instituto de Fisica, Avenida Bento Gonçalves 9500, 91501-970 Porto Alegre, RS, Brazil

[*] corresponding author, email: d.p.woodruff@warwick.ac.uk

1. Introduction

The interaction of alkanethiols ($CH_3(CH_2)_{n-1}SH$) with noble metal surfaces, Au, Ag and Cu, and particularly with Au(111), has attracted very considerable interest, being an archetypal self-assembled monolayer (SAM) system with a wide range of actual and potential applications (e.g. [1, 2, 3, 4]). Despite this, our current state of understanding of the structure of the interface between the metal surface and the S head-group is poor, even in the much-studied case of the Au(111) substrate. The simplest alkanethiol is methanethiol, CH_3SH, and although the absence of a long alkane chain must clearly influence the intermolecular interactions within the adsorbed layers, this species is the most tractable for *ab initio* total energy calculations. Like the longer-chain alkanethiols, methanethiol deprotonates on these surfaces to form an adsorbed methylthiolate (CH_3S-) species; this same surface species can also be formed be exposure to dimethyldisulphide – DMS – $(CH_3S)_2$ – through S-S bond scission at the surface. In part because of the relative simplicity of dealing with methanethiolate theoretically, and in part because UHV (ultra-high vacuum) dosing of DMS or methanethiol is straightforward, this species has been subjected to the largest number of structural studies.

On Cu(111), methylthiolate is known to induce a major reconstruction of the outermost metal layer [5, 6, 7]. On Au(111) it has generally been supposed that no such reconstruction occurs, and that the ordered ($\sqrt{3}$x$\sqrt{3}$)R30° phase formed is a simple overlayer. However, fundamental inconsistencies between the preferred adsorption site found in theoretical calculations for this phase (hollow or bridge) with those found experimentally using two entirely different structural techniques (photoelectron diffraction [8] and NIXSW (normal incidence X-ray standing waves) [9]) (atop) has led to the suggestion that the Au(111) surface may also be reconstructed by the adsorbed thiolate [9], leading to a surface structure untested by theoretical calculations.

On Ag(111), methylthiolate forms a ($\sqrt{7}$x$\sqrt{7}$)R19°-CH_3S surface phase which, like the alkylthiolate SAMs on Au(111), seems to have been implicitly supposed to correspond to

a simple adsorbed overlayer on an unreconstructed surface. Indeed, the only theoretical total energy calculations of the Ag(111)/CHS$_3$S system assumes the surface is unreconstructed and fail to consider the coadsorbed multiple site occupation implied by the ($\sqrt{7}$x$\sqrt{7}$) adsorption phase [10, 11]. However, in this case recent scanning tunnelling microscopy (STM) [12] and NIXSW [13] studies have provided indirect evidence that, like Cu(111), this surface is also strongly reconstructed. The favoured structural model has an outermost Ag layer containing only 3/7 the coverage of Ag atoms of the underlying bulk layers. The STM imaging showed evidence of substantial movement of Ag surface atoms, and probable ejection of Ag atoms from the outermost layers during the thiol reaction, consistent with a density-lowering Ag surface reconstruction. STM also provided atomic-scale images interpreted in terms of three thiolate species per ($\sqrt{7}$x$\sqrt{7}$) surface mesh. The NIXSW measurements provided information on the location of the S atoms relative to the extended underlying Ag bulk lattice that were shown to be incompatible with adsorption on an unreconstructed surface, and consistent with a specific model of the reconstruction, but gave no direct information on the location of the Ag atoms.

To provide more direct evidence of the Ag(111) surface layer reconstruction induced by methylthiolate adsorption, we present here the results of an investigation using medium energy ion scattering (MEIS). The MEIS technique [14], in which typically 100 keV H$^+$ ions are scattered from the surface, is a variant of the standard method of Rutherford backscattering, but the somewhat lower ion energies allow the use of electrostatic dispersive ion energy analysers that have much better energy resolution. As the inelastic energy loss is proportional to the distance travelled by the ions in the solid, this improved energy resolution is translated into improved depth resolution. In the present case, however, we exploit the elastic scattering shadow cones on the incident trajectory to illuminate only a very small number of near-surface atomic layers. A further key aspect of MEIS for our present investigation is the ability to determine in an *absolute* fashion the number of layers contributing to the scattered signal. In particular, if reconstruction leads to atoms of the substrate species being displaced away from their positions in an ideal bulk-terminated surface, this gives rise to an enhanced scattering signal that can be

quantified in terms of the number of such displaced atoms. It is this aspect of MEIS, in particular, that provides the potential to obtain valuable new complementary information regarding the possible thiolate-induced reconstruction of the Ag(111) surface, in the same way that this information was obtained for the quite different thiolate-induced reconstruction of Cu(111) [7].

2. Experimental Details

The experiments were performed at the Daresbury Laboratory UK National MEIS facility [15]. The ion accelerator fitted with a duoplasmatron ion source was used in the present experiments to produce a beam of H^+ ions at a nominal energy of 100 keV. The end-station comprises separate UHV chambers for sample preparation and characterisation, for sample storage, and for the ion scattering experiments, with sample transfer between chambers being achieved under UHV conditions. The Ag(111) sample was prepared *in situ* by the usual cycles of 1 keV argon ion bombardment and annealing (550°C, 15 minutes) until a well-ordered clean surface was obtained as judged by a sharp (1x1) low energy electron diffraction (LEED) pattern and Auger electron spectroscopy. The methanethiolate adsorbate layer was prepared by exposing the surface to typical partial pressures of 10^{-8}-10^{-7} mbar of dimethyldisuphide (CH_3S-SCH_3) at room temperature, introduced into the preparation chamber through a leak valve from a glass ampoule, first subjected to several freeze-thaw pumping cycles. An exposure of $6x10^{-6}$ mbar.s appeared to be sufficient to achieve saturation coverage, but MEIS measurements were also taken after exposures an order of magnitude larger with no significant difference in the resulting coverage. LEED showed the formation of the expected ($\sqrt{7}x\sqrt{7}$)R19° pattern, although in view of the known susceptibility of this surface to radiation damage, the conditions to obtain the ordered overlayer phase were first conducted with the aid of LEED, but thereafter LEED patterns were recorded from samples only after MEIS data collection.

MEIS measurements were performed with the sample at room temperature. The sample was aligned with respect to the incoming ion beam by means of a high-precision

goniometer. Incident ion doses, measured by means of a 71% transparent tungsten mesh mounted in the beam path, were limited to 10 μC total charge onto a single area of the surface; with a sample spot size of 1 x 0.5 mm^2 this corresponds to a total of ~10^{16} ions. cm^{-2}. Data collected with total charge input of 2.5 μC and 5.0 μC differed only in the level of statistical noise, indicating that there was no detectable ion-induced damage to the sample. Ions scattered from the sample were detected by a moveable toroidal electrostatic analyser, the two-dimensional detector [16] of which provides 'tiles' of ion counts as a function of both ion energy and scattering angle over limited ranges of each. Additional measurements at slightly different pass energies or angular positions allowed several such tiles to be joined together to provide more extensive two-dimensional energy and angular maps. Subsequent processing allowed integration of the scattered ion intensity over selected ranges of energy or angle to provide either blocking curves or ion energy spectra, respectively. These methods of data reduction have been described elsewhere [15, 17], although the blocking curves (angular dependence of the Ag surface scattering peak) were extracted by a superior method developed more recently that is based on fitting the surface peak in the scattered ion energy spectrum, at each scattered angle channel, to an asymmetric Gaussian and a background [7].

An important aspect of the present study was to have a reliable calibration of the absolute scattering yield from the surface, and to achieve this measurements were made on a reference sample of Cu shallowly implanted in Si to a known concentration (3.12x10^{15} atoms.cm^{-2} with a precision of ±3%), established independently by conventional Rutherford backscattering. An implicit assumption in using this reference sample is that the scattered ion charge fraction (known to be very high in general for 100 keV H$^+$ scattering) is essentially identical for the reference and Ag(111) surface samples.

3. Experimental results and theoretical simulations

Fig. 1 summarises the final results of the experiment, namely the blocking curves from the MEIS scattered ion signal from Ag atoms contributing to the 'surface peak' in the scattered ion energy spectra. Two different incident directions were used for these

measurements, namely [$1\bar{1}0$], corresponding to nominal one-layer illumination (i.e. a direction in which the surface layer Ag atoms of an ideal bulk-terminated surface shadow all sub-surface atoms) and [$\bar{1}\bar{1}2$], which corresponds to a nominal two-layer illumination (Ag atoms below the second layer being shadowed by atoms in one of the outermost two layers). In reality, of course, some deeper-lying atoms are illuminated in both of these geometries due to the effects of thermal vibrations and possible surface layer relaxations. On the other hand, in some outgoing directions ions scattered from sub-surface atoms are blocked from reaching the detector by surface atoms, so even in the nominal two-layer illumination geometry ([$\bar{1}\bar{1}2$]) the scattered ion yield in the deepest blocking dips corresponds to a signal from less than two layers.

As remarked above, absolute calibration of the scattered ion yield is an important feature of the MEIS technique, because this allows one to express the scattered ion yield in terms of the number of Ag atoms per unit area that contribute to the signal, shown in fig. 1 as the number of Ag layers. Our use of the Cu-implanted Si sample provides a convenient absolute reference, but a further check comes from a comparison of the measured blocking curves from the clean Ag(111) surface with the results of a simulation of the scattering from this surface using the VEGAS computer code [18] in which the scattering is described by a Thomas-Fermi-Molière potential and the effect of thermal vibrations is accounted for using a Monte Carlo algorithm. These calculations yield predictions for the number of Ag layers contributing to the scattered ion yield as a function of incident and collection directions that can be compared directly with the measured blocking curves. Of course, these absolute yields are influenced by the magnitude of the thermal vibrations, more subsurface layers contributing to the signal as the vibrational amplitudes increase and the possibility of ions not being shadowed or blocked increases. In Fig. 1 the full lines through the experimental clean surface data are the results of VEGAS simulations in which the fit to the experiment has been optimised (through minimisation of a suitable reliability- or *R*-factor [19]) by adjusting the surface layer vibrational amplitudes. Note that in order to avoid weighting the parts of the blocking curves at small scattering angle (where the scattering cross-sections are greatest) the theory-experiment comparisons were performed on the data divided by the angular dependence of the scattering cross-

section (i.e. on the data as presented in fig. 1). No surface inter-layer spacing relaxation was included in these calculations, consistent with an exact alignment of the surface and bulk blocking dips and many previous studies of metal fcc (111) surfaces showing essentially negligible surface relaxations. In minimising the *R*-factor the scaling factor relating the scattered ion yield in detected ions to the number of layers contributing was allowed to vary by up to 5% relative to the value given by the Cu-implanted Si reference sample. This actually represents a somewhat tighter constraint than the value of 10% often used in MEIS studies. Using rms (root-mean-square) vibrational amplitudes for the bulk Ag atoms of 0.09 Å, obtained from the bulk Debye temperature (225 K), the optimised values of the enhanced rms vibrational amplitudes perpendicular to the surface for the outermost and second surface layers were found to be 0.16 Å and 0.14 Å respectively, in broad agreement with expectations. We should note that the absolute scattering yields are also dependent on the crystalline quality of the near-surface region. In our first experiments on a new Ag(111) sample, prepared by the usual combination spark-machining, mechanical polishing, and subsequent argon ion bombardment and annealing in the UHV chamber, we found significantly higher average scattering yields that led to an inconsistency between the calibrations based on the reference sample and on the VEGAS simulations of the Ag blocking curves. The data shown here are from a sample that had gone through many more argon ion bombardment and annealing cycles over several months of use in other thiol and sulphur dosing experiments, a process that evidently removed the subsurface region damaged in the mechanical cutting and polishing process, leading to good agreement for the alternative means of calibration.

Fig. 1 also shows the blocking curves obtained from the Ag(111)($\sqrt{7}$x$\sqrt{7}$)R19°-CH$_3$S surface. In both incident directions there is a significant enhancement of the Ag scattering signal, a clear indication that some near-surface Ag atoms have been displaced significantly from their bulk positions as a result of the formation of the thiolate layer. In order to quantify this effect further, however, it is necessary to explore specific structural models. Fig. 2 shows models of the surface considered in earlier studies, notably in (a) the basic model without Ag(111) surface layer reconstruction and in (b) two alternative reconstructed surface models [12, 13]. In each case the coverage of the thiolate is

believed to be 3/7 ML, or three thiolate species per (√7x√7) unit mesh, consistent with the √(7/3) periodicity of the protrusions seen in STM. In the absence of any Ag surface reconstruction (fig. 2(a)) this periodicity is consistent with the three thiolate species within the unit mesh occupying the two inequivalent hollow sites ('fcc' directly above a third layer Ag atom and 'hcp' above a second layer Ag atom) and atop sites, but such a model implies a large height variation of the thiolate species in the atop and hollow sites, a feature apparently inconsistent with both the STM and NIXSW data. Fig. 2(b) shows two possible reconstruction models that have the potential to alleviate this inconsistency, involving outermost Ag layers of reduced atomic density of either 4/7 ML or 3/7 ML. In the 3/7 ML Ag model, in its simplest form as shown in fig. 2, all the thiolate species are coplanar. Both the STM and NIXSW data favour this 3/7 ML model, but with a slight lateral distortion of this model such that the Ag atoms in the reconstructed layer are displaced slightly towards the nearest hollow sites on the underlying unreconstructed Ag(111) layer. This lateral distortion of the Ag atoms of ~0.14 Å in the 3/7 ML reconstructed layer causes the thiolate species atop Ag atoms in the outermost unreconstructed Ag layer to be displaced outwards from the surface relative to the thiolates above the substrate hollow sites, leading to a rumpling of the thiolate layer of ~0.4 Å. This amplitude of rumpling was proposed to give the best fit to the NIXSW data [13]. Note that one feature of this model is that all the thiolate species occupy three-fold coordinated hollow sites relative to the reconstructed Ag surface layer.

Fig. 1 shows the results of VEGAS calculations based on these two models, in each case assuming the interlayer spacings in the surface Ag and CH_3S layers are based on hard-sphere models with metallic Ag radii and Ag-S nearest-neighbour distances of 2.70 Å. In these calculations only the relatively strongly-scattering S atoms are included to represent the influence of the adsorbed thiolate species on the blocking curves. The location of the methyl (CH_3) groups is not known (the S-C bonds are probably tilted relative to the surface normal) but as both C and H atoms are very weak scatterers their omission from the VEGAS calculations is unlikely to have any significant consequences. The results for the 3/7 ML Ag layer in fig. 1 correspond to the simple model as shown in fig. 2 without lateral distortion of this Ag layer. Notice that because of the reduced symmetry of these

overlayer structures, the simulations are the average of the results of VEGAS calculations for two inequivalently rotated domains related by the substrate mirror symmetry planes. In conducting these simulations it is necessary, once again, to establish the appropriate vibrational amplitudes. In particular, because the outermost unreconstructed Ag layer is no longer the surface layer, the vibrational amplitudes for this layer were set to the bulk values. This same procedure was found to be consistent with MEIS results for the thiolate-induced reconstruction of the Cu(111) surface [7]. Fortunately, the value of the vibrational amplitudes for the Ag atoms in the reconstructed layer (which are completely unknown), prove to be unimportant; because these atoms are well-removed from bulk positions, they cause rather little shadowing or blocking of scattering from lower layers, and this is insensitive to the vibrational amplitudes. One consequence of this modification of the surface layer vibrations is that the effect of adding 3/7 ML or 4/7 ML of displaced Ag atoms to the Ag(111) surface is *not* a simple addition of 3/7 or 4/7 of a layer to the scattered ion yield. This effect is most noticeable for the [$\bar{1}\bar{1}0$] incidence data. In this geometry the substrate shadowing nominally only illuminates the outermost layer, but in fact, away from the blocking dips, the signal from the clean surface corresponds to scattering from ~1.65 layers, a direct consequence of the large vibrational amplitudes associated with the low Debye temperature of Ag. Reducing the vibrational amplitudes of the complete outermost Ag layer to the bulk value thus leads to a reduced signal from the subsurface, so adding 3/7 ML of extra Ag atoms leads to an average enhancement of the scattering relative to the clean surface of only about 0.25 layers, compared with the expected value of 0.43 (3/7) layers. By contrast, for [$\bar{1}\bar{1}2$] incidence, a direction in which the Ag atoms in the bulk are more widely spaced and thus sit in wider shadow cones, the effect of these changes to the surface vibrations is much less pronounced.

Evidently the experimental data of fig. 1 show clear evidence for thiolate-induced reconstruction of the Ag(111) surface, and comparison with the simulations for the two model structures also shows substantially better agreement with the 3/7 ML Ag model for [$\bar{1}\bar{1}0$] incidence. In the [$\bar{1}\bar{1}2$] incidence direction, the Ag atoms in the reconstructed 4/7 ML do cause some shadowing (~0.1 layers) of the substrate, so the difference in the absolute scattering yields for the two models are rather similar. Clearly the [$\bar{1}\bar{1}0$]

incidence data are more sensitive to the structural model and we focus on these data in considering structural refinements. Fig. 3 shows a comparison of the experimental blocking curve recorded in [1̄1̄0] incidence from the thiolate-covered surface with three structural variations of the basic 3/7 ML Ag overlayer model. In particular, both the STM and NIXSW experiments have been interpreted in terms of some rumpling of the thiolate layer, so in addition to the simulations for the simple coplanar layer model expected from fig. 2, fig. 3 shows results for the 'relaxed' version of this model proposed on the basis of the NIXSW experiments which incorporates a rumpling of 0.4 Å and the associated 0.14 Å lateral distortions of the reconstructed Ag layer. Notice that because the Ag atoms in this layer are in low symmetry sites the lateral distortion has no detectable effect on the MEIS blocking curves. Interestingly, this more refined model actually appears to fit the experimental MEIS data significantly less well than the simple coplanar model. In particular, all three of the major blocking dips at ~71°, ~77° and 90° (corresponding to [1̄1̄4], [1̄1̄6] and [001] outgoing directions) are slightly displaced in angle relative to the experimental data. The reason for this turns out to be the effect of blocking of scattering from the outermost unreconstructed Ag(111) layer by the S atoms of the thiolate species. While the reconstructed Ag layer atoms are well-removed from high-symmetry sites, and thus have little influence in shadowing or blocking the substrate scattering, the S atoms are in high-symmetry sites and so can have a significant effect.

To illustrate this more clearly we have evaluated the contributions in the VEGAS simulations to this blocking curve from the individual Ag atomic layers. These individual layer contributions are expressed in terms of layer-dependent hitting probabilities, the sum of these hitting probabilities for the various layers being the total number of contributing layers, the quantity plotted in figs 1 and 3. Notice that the VEGAS program determines the scattered ion signal by determining the product of the probability that a specific atom will be hit by the incoming ions and the probability that the same atom would be hit if the ions entered along the direction of the measured outgoing scattered ions. This simple use of time-reversal symmetry leads to the vocabulary 'hitting probability', although bearing in mind that the second of these hitting probabilities is actually evaluating the effect of outgoing ion blocking, this product should perhaps more

10

appropriately be referred to as 'visibility probability' or 'scattering probability'.

Fig. 4 shows the results of these layer-dependent hitting probabilities for the simple 3/7 ML Ag reconstruction model with coplanar thiolate species. The reconstructed 3/7 ML Ag layer itself contributes exactly 3/7 (0.43) layers to the signal, with no evidence of blocking by the S atoms that lie above. The second and third complete Ag(111) substrate layers shows the expected bulk blocking dips associated with scattering by the complete Ag layer(s) above, with the second layer having a hitting probability of ~0.4 layers away from the blocking dips, while the third layer is far more effectively shadowed by the outer layers and contributes only ~0.05 layers of scattered ion signal. The outermost complete Ag layer, however, shows blocking dips due to the influence of the S atoms in the thiolate overlayer that are in high-symmetry registry sites. Surprisingly, the average yield from this layer is actually slightly in excess of 1 layer. A detailed breakdown of the VEGAS results reveals that this is due to the fact that while these Ag atoms lie outside the shadow cones of the Ag atoms in the reconstructed layer, they lie sufficiently close to these shadow cones that they experience some focussing of the incident beam on the edge of the shadow cones. Of particular significance in this hitting probability curve for the outermost layer is the absence of significant blocking features around the bulk [$\bar{1}\bar{1}4$] blocking at ~71°, and the presence of a blocking dip very close to the [001] 90° bulk blocking dip. The angular coincidence of these two features is attributable to blocking by the S atoms in atop sites relative to this unreconstructed layer that happen to lie almost exactly 1.5 bulk layer spacings above.

By contrast the 'relaxed' version of this 3/7 ML Ag reconstruction model, incorporating lateral distortion of the reconstructed Ag layer and a resultant 0.4 Å rumpling of the thiolate layer, as favoured by the previous NIXSW investigations, leads to significant differences in this outermost layer hitting probability curve, as shown in fig. 5 which compares only this one layer contribution in the 'simple' and 'relaxed' models, and in a further variant described below. The rumpling in the layer means the S atoms in the atop sites relative to outermost unreconstructed layer are moved up, shifting the associated blocking dip near 90° to higher angle, while the S atoms above the hollow sites move

11

down, causing the blocking dips associated with these S atoms to move to low scattering angles. It is these shifts, and the enhanced blocking dips at smaller scattering angles, which lead to the poorer agreement seen in the complete blocking curve calculation of fig. 3.

Evidently, these relatively weak blocking features of the outermost substrate layer by the S atoms can have a significant influence on the exact angles and depths of the MEIS blocking dips. For the 'simple' coplanar thiolate model with a layer spacing relative to the substrate consistent with the NIXSW measurements of ~1.5 substrate layer spacings the agreement in the angles and relative depths of the blocking dips is generally good, whereas for the 0.4 Å rumpled 'relaxed' model, it is very significantly less good. Figs 3 and 5 also show the results of calculations for essentially the same model in which the rumpling amplitude is reduced to 0.2 Å. In this case the relative good agreement with experiment is recovered, and indeed the shape of the blocking curve around scattering angles of ~75-82° is somewhat improved.

4. General discussion and conclusions

The theory-experiment blocking curve comparisons of fig. 1 clearly show that the formation of $Ag(111)(\sqrt{7}x\sqrt{7})R19°-CH_3S$ surface phase is accompanied by significant rearrangement of the Ag surface atoms, and indeed that the number of displaced Ag atoms is in quite good agreement with the expectations for the 3/7 ML Ag reconstruction model and in poor agreement with the model based on 4/7 ML of displaced Ag atoms. The more detailed analysis of the blocking curve recorded with $[\bar{1}\bar{1}0]$ incidence, that is seen to be most sensitive to the details of the structural model, is also found to favour somewhat weaker rumpling of the thiolate layer than had previously been suggested on the basis of, in particular, the earlier NIXSW experiments.

Two key questions remain, namely, why are the theoretical simulations for the $[\bar{1}\bar{1}0]$ incidence data rather consistently about 0.1 layers higher in yield than the experimental ones, and can we reconcile the apparent preference for relatively weak corrugation of the

thiolate layer with the results of the earlier STM and NIXSW experiments?

Evidently the first of these questions raises the issue of the precision of the absolute yield measurements. As remarked above, MEIS yields are typically regarded as accurate to about ±10%, significantly larger than the discrepancy here which is approximately 5%. However, one would expect the *relative* yields of the clean and reconstructed Ag surfaces to be reliable to substantially better than 10%, so the discrepancy does appear to be significant. Perhaps the most obvious source of this discrepancy concerns the value of the vibrational amplitudes of the Ag atoms in the bulk and in the outermost layer of the clean surface. As noted earlier, the clean surface data and associated VEGAS calculations form the basis of the absolute yield calibration, supported by the independent measurements of the Cu-implanted Si sample that agree to within 5%. For the clean surface, the magnitude of the enhanced vibrational amplitudes of the outermost surface layer(s) has the largest impact on the absolute scattering yields, particularly for $[\bar{1}\bar{1}0]$ incidence, because this parameter influences the extent to which the second substrate layer contributes to this yield. For the reconstructed surface, on the other hand, we assume that the vibrational amplitudes of the Ag atoms in the outermost unreconstructed layer are not enhanced relative to the bulk, and while the Ag atoms in the 3/7 ML reconstructed layer probably do have enhanced vibrations, the low-symmetry location of these atoms means that their vibrational amplitudes have a negligible effect on the visibility of the lower layers. For this surface, therefore, it is the amplitude of the bulk atomic vibrations that mainly influence the contribution of deeper-lying sub-surface atoms to the scattered ion yield. In principle, of course, the bulk vibrational amplitudes are well known from the measured Debye temperature, but the value of this parameter obtained from different methods (e.g. X-ray diffraction and specific heat measurements) does vary, and in MEIS studies of Cu(111) and Ni(111), Kido and co-workers [20] have shown that the different tabulated Debye temperatures do lead to significant variations in the predicted ion yield. For Ag original measurements of the Debye temperature do show some variation, with some quoted values being both lower (e.g. [21]) and (slightly) higher (e.g. [22, 23]) than the standard text-book value used here of 225 K [24]. For our present study we note that larger surface vibrational amplitudes of the clean surface, or smaller bulk vibrational

amplitudes would bring the theoretical yields of the clean and thiolate-covered surfaces closer together, thus reducing the observed discrepancy with experiment. The relative size of the surface and bulk vibrations found in our clean-surface fitting routine is at the upper end of the expected range, so larger values seem unlikely. The highest published values of the bulk Debye temperature are only slightly larger than the value we have used to determine the bulk vibrational amplitudes, so it seems unlikely that an error in this parameter is the source of the discrepancy. On the other hand, one factor that is not included in our calculations is the influence of correlations in the vibrations of nearest-neighbour atoms (see, e.g [20]). Including this effect in the scattering from the reconstructed surface would enhance the shadowing of the sub-surface layers and thus lead to a reduced scattering yield; it is therefore possible that this omission could account for the discrepancy in absolute scattering yield from the reconstructed surface.

Finally, we consider the issue of the rumpling of the thiolate layer on the reconstructed Ag surface. The MEIS results show that an unrumpled layer, as expected from a simple hard-sphere model on a perfectly periodic reconstructed 3/7 ML Ag layer is compatible with the experimental data, whereas a similar structure with a significant (0.4 Å) rumpling fits significantly less well. The MEIS data thus clearly favour a smaller rumpling amplitude. The notion of a rumpled layer arises from two pieces of evidence. Firstly, STM images [12] show a height variation of the protrusions attributed to the thiolate species, although this is sensitive to tip condition. In some images all the protrusions are of similar height, in others only one of the three potential protrusions per ($\sqrt{7}$x$\sqrt{7}$) unit mesh is seen, and in other images a height difference of about 0.3 Å is seen, with one protrusion per unit mesh higher than the other two. Of course, STM is a probe of electronic structure, not the positions of the atomic centres, as highlighted by the different images obtained under different conditions. It is therefore perfectly possible that the true corrugation is either significantly greater or smaller than the measured 0.3 Å in the highest-resolution images. Indeed, the observed height variation could be entirely electronic in origin, as the local structural environments of the three thiolate species in each unit mesh are different.

The second piece of evidence favouring a rumpled thiolate layer comes from the NIXSW experiments [13]. In this case the key parameters indicating rumpling are the so-called coherent fraction values for the different standing wave conditions. For the 'simple' 3/7 ML Ag reconstruction model, with coplanar thiolate species, one expects the coherent fraction for the (111) standing waves, in this case effectively an order parameter, to be close to unity ('perfect order' perpendicular to the surface), while the equivalent parameter for standing wave nodal planes not parallel to the surface should be identically zero. Experimentally, the (111) coherent fraction was found to be 0.72, while the values for the other standing wave conditions were small (~0.10) but apparently non-zero. A rumpling amplitude of ~0.4 Å was found to give a somewhat better account of the measured coherent fractions. However, if the reduced (111) coherent fraction is due, in part, to some form of disorder, the NIXSW data could also be consistent with a much smaller (possibly even zero) rumpling amplitude.

In conclusion, the present MEIS experiments provide the first *direct* evidence that the Ag(111)($\sqrt{7} \times \sqrt{7}$)R19°-CH$_3$S surface phase does involve substantial reconstruction of the Ag surface layer, and is generally good agreement with a specific model based on a reconstructed layer containing 3/7 ML Ag atoms, clearly favouring this over an alternative model based on a 4/7 ML reconstructed Ag layer. In general this conclusion is in excellent agreement with previous reports of this reconstruction based on STM and NIXSW experiments. However, the MEIS data indicate that any rumpling of the thiolate layer, previously proposed on the basis of these earlier studies, is small,and probably ≤ 0.2 Å. While smaller than the amplitude suggested in these earlier studies, such a value could be entirely consistent with the experimental results of these STM and NIXSW studies.

Acknowledgements

Figure Captions

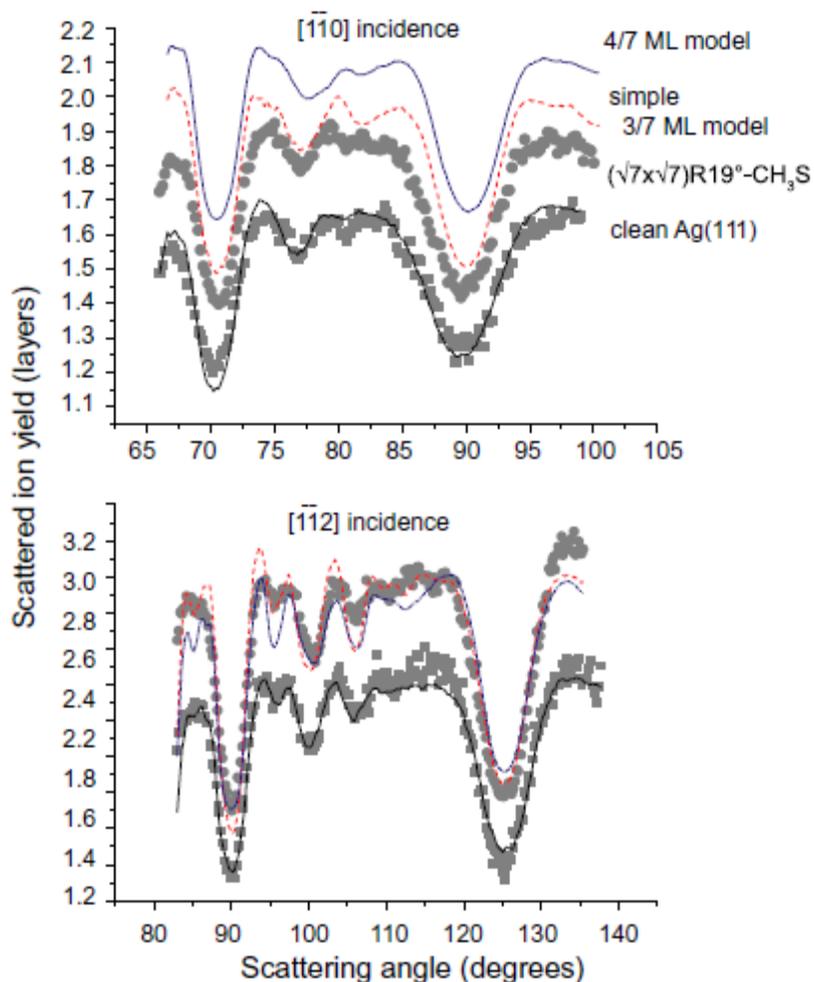

Fig. 1 100 keV H^+ MEIS blocking curves from clean Ag(111) and Ag(111)($\sqrt{7}$x$\sqrt{7}$)R19°-CH_3S surfaces and two different incidence geometries. The experimental data are shown as individual data points (squares for the clean surface, circles for the thiolate-covered surface). The full lines are the results of theoretical simulations for the clean surface, while the dotted and dashed lines are the results of similar simulations for the two structural models of the thiolate-covered surface shown in fig. 2.
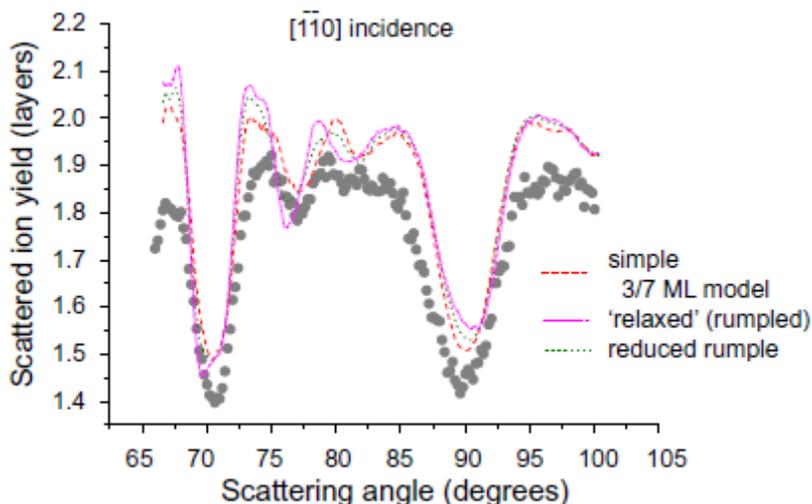
Ag(111)(√7x√7)R19.1°-CH$_3$S   S coverage 3/7 ML

a   unreconstructed

b   reconstructed

Ag coverage 4/7 ML   Ag coverage 3/7 ML

Fig. 2 Schematic diagrams of models of the Ag(111)(√7x√7)R19°-CH$_3$S surface structure discussed in previous publications. In (a) is shown the basic model based on adsorption on an unreconstructed Ag(111) surface, while (b) shows two alternative reconstruction models. In each case the light-shaded circles represent Ag atoms in the unreconstructed substrate, the Ag atoms of the reconstructed outermost layer are shown in intermediate shading and the S atoms of the thiolate species are shown as small dark-shaded circles. The lines show the (√7x√7)R19° unit mesh.

Fig. 3 Comparison of the experimental 100 keV H$^+$ MEIS blocking curves (circles) from Ag(111)($\sqrt{7}$x$\sqrt{7}$)R19°-CH$_3$S in [$\bar{1}\bar{1}0$] incidence with the results of VEGAS simulations for three variants of the 3/7 ML Ag reconstruction model as described in the text.
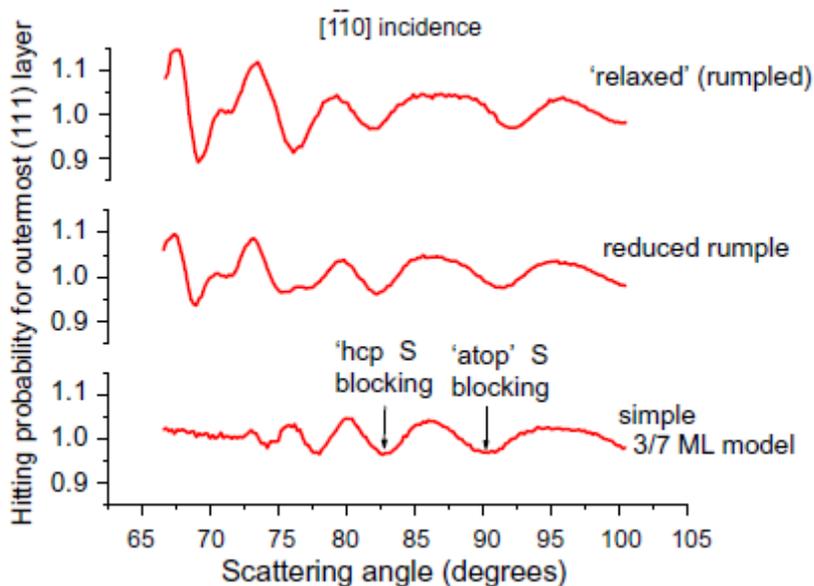

Fig. 4 Blocking curves in [$\bar{1}\bar{1}0$] incidence of hitting probabilities for the outermost Ag atomic layers in the simple 3/7 ML Ag reconstruction model (with coplanar thiolate molecules) of the Ag(111)($\sqrt{7}$x$\sqrt{7}$)R19°-CH$_3$S surface as calculated by VEGAS.
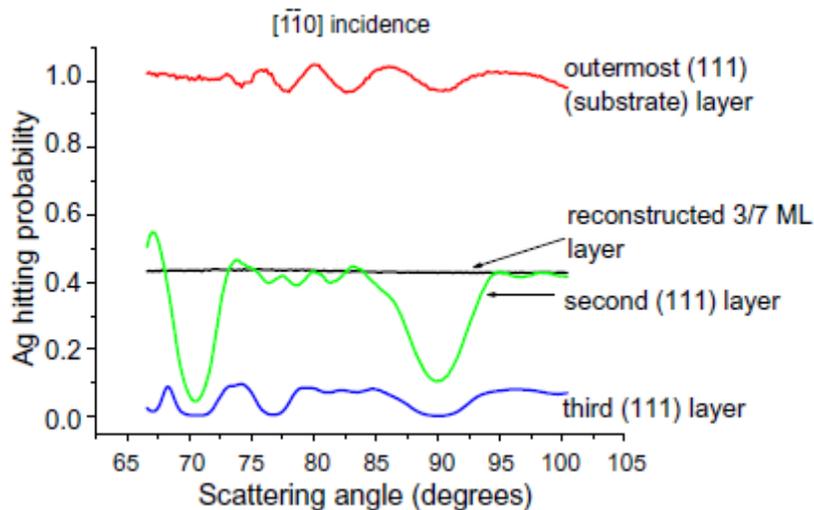
18

Fig. 5 Comparison of blocking curves in [$\bar{1}\bar{1}0$] incidence of hitting probabilities for the outermost unreconstructed Ag atomic layer in three different forms of the 3/7 ML Ag reconstruction model of the Ag(111)($\sqrt{7}$x$\sqrt{7}$)R19°-CH_3S surface as calculated by VEGAS. The dips associated with blocking of the outgoing ions by the S atoms in the atop and hcp sites relative to the underlying Ag(111) substrate are labelled.

References

1 L. H. Dubois, R. G. Nuzzo, Annu. Rev. Phys. Chem. 43 (1992) 437

2 A. Ulman, Chem. Rev. 96 (1996) 1533

3 F. Schreiber, Prog .Surf. Sci. 65 (2000) 15.

4 J. C. Love, L. A. Estroff, J. K. Kriebel, R. G. Nuzzo, G. M. Whitesides. Chem. Rev. 105 (2005) 1103

5 G. J. Jackson, D. P. Woodruff, R. G. Jones, N. K. Singh, A. S. Y. Chan, B. C. C. Cowie, V. Formoso, Phys.Rev.Lett. 84 (2000) 119

6 S.M.Driver and D.P.Woodruff, , Surf.Sci. 457 (2000) 11

7 G. S. Parkinson, M.A. Muñoz-Márquez, P.D. Quinn, M. Gladys, D.P. Woodruff, P. Bailey, T.C.Q. Noakes, Surf. Sci. 598 (2005) 209

8 H. Kondoh, M. Iwasaki, T. Shimada, K. Amemiya, T. Yokohama, T. Ohta, M. Shimomura, K. Kono., Phys. Rev. Lett. 90 (2003) 066102

9 M. G. Roper, M. P. Skegg, C. J. Fisher, J. J. Lee, V. R. Dhanak, D. P. Woodruff, R. G. Jones, Chem. Phys. Lett. 389 (2004) 87.

10 H. Sellers, A. Ulman, Y. Shnidman, J. E. Eilers, J. Am. Chem. Soc. 115 (1993) 9389

11 F. P. Cometto, P. Paredes-Olivera, V. A. Macagno, E. M. Patrito, J. Phys. Chem. B 109 (2005) 21737

12 Miao Yu, S.M. Driver and D.P. Woodruff, Langmuir 21 (2005) 7285

13 Miao Yu, D.P.Woodruff, N. Bovet, C.J. Satterley, K. Lovelock, Robert G. Jones, V. Dhanak, J. Phys. Chem. B 110 (2006) 2164

14 J.F. van der Veen, Surf. Sci. Rep. 5 (1985) 199

15 P.Bailey, T.C.Q. Noakes and D.P. Woodruff, Surf. Sci. 426 (1999) 358

16 R.M. Tromp, M. Copel, M.C. Reuter, M. Horn von Hoegen, J. Speidell and R. Koudijs, Rev. Sci. Instrum. 62 (1991) 2679

17 D. Brown, T.C.Q. Noakes, D.P. Woodruff, P. Bailey, Y. Le Goaziou, J. Phys.: Condens. Matter 11 (1999) 1889

18 R.M. Tromp and J.F. van der Veen, Surf. Sci. 133 (1983) 159

19 G. S. Parkinson, M. A. Muñoz-Márquez, P. D. Quinn, M. J. Gladys, R. E. Tanner, D. P. Woodruff, P. Bailey, T. C. Q. Noakes, Phys. Rev. B 73 (2006) 245409

20 T. Okazawa, F. Takeuchi, Y. Kido, Phys. Rev. B 72 (2005) 075408

21 M. Simerská, Acta Cryst. 14 (1961) 1259

22 J. R. Neighbours, G. C. Alers, Phys. Rev. 111 (1958) 707

23 D. L. Martin, Phys. Rev. B 8 (1973) 5357

24 C. Kittel, Introduction to Solid State Physics, 7th Edition, John Wiley & Sons, New York, 1996